Doppler boosting effects on relativistic jets

Author: Víctor E. López Arias.
Advisor: Valentí Bosch-Ramon
Facultat de Física, Universitat de Barcelona, Diagonal 645, 08028 Barcelona, Spain.*

Abstract: The following work is focused on the study of the Doppler boosting effects on relativistic jets -*i.e.* those found in Active Galactic Nuclei (AGN). The scope of this research is to provide an exploration of the effects caused by the relativistic Doppler boosting effect on the apparent luminosity of relativistic jets in AGN as perceived by an external observer, as relativistic motion and flow orientation are important factors in the observed emission. Representative parameters and reasonable approximations have been used to simplify the calculations in order to present a simple but instructive model of these relativistic jets.

I. INTRODUCTION

Relativistic jets are collimated outflows of plasma and fields formed from accretion processes in compact objects. This accreted matter is ionized and thus produces non-thermal radiation, ranging from radio to gamma-rays. The jet phenomenon appears commonly in central objects onto which matter is accreted from the surrounding environment, becoming relativistic when the central object is compact. Some examples of such a behaviour are neutron star and black hole binaries in galactic systems, and active galactic nuclei (AGN) or gamma-ray bursts (GRB) in extragalactic systems [1].

The plasma that forms the jets emits non-thermal radiation, usually described as a result of synchrotron radiation- *i.e.* the radiation produced by the spinning particles at ultra-relativistic speeds around the magnetic field, or by means of inverse Compton effect. Namely, the scattering of low energy photons to high energies transferred from electrons with high kinetic energy. These processes are described in detail in [2].

Relativistic jets are embedded in rich environments, and stars and dense medium inhomogeneities can enter into these jets leading to the formation of shocks. Due to the strong pressure gradient in the shock jet material, the flow can again be accelerated to relativistic speeds even when they are close to a certain obstacle [3]. A simple representation of these situations is the one presented in this work: first, a conical jet is considered. Then the interaction is modelled as a conical jet until it reaches the obstacle. The jet starts as a conical form with a plain base, growing in size in the same conical shape until it reaches the obstacle. After the interaction with the obstacle, the deflected fluid lines are modelled as forming a paraboloid. This paraboloid structure contains the same total amount of segments than the jet without the obstacle, but now concentrated solely in its surface. A sketch of these scenarios mentioned is shown in Figure 1.

The relativistic Doppler boosting effect is a well-known phenomenon in physics. Doppler boosting modifies the apparent luminosity of emitting matter, the jet plasma, due to its relativistic velocity. This phenomenon determines the angular distribution of the radiated emission in the laboratory frame of reference, and thus, the observer's line of sight determines the apparent luminosity [4], [5]. This study is focused on how this change induced in the apparent luminosity evolves when varying the relativistic and geometrical properties of the jet.

Relativistic jets are usually studied as fluids, and in this case, it is assumed that the jet is stationary. Thus, this leads into a continuous steady pattern in which the radiation is emitted in an isotropic manner in the flow frame. Then one can divide the emitting flow into lines of emission to study the jet, *i.e.* like a fluid is divided into fluid lines. These lines are subsequently divided into segments with certain properties of orientation, emitted radiation and velocity.

For simplicity, here it is assumed that all these segments have the same luminosity in the flow frame, and the same 3-velocity modulus. Such former velocities are at an angle θ to the observer's line of sight, which is defined as the angle between the observer and the orientation of each segment. This can be seen in detail in Figure 2. The following sections will contain a detailed explanation of the physical model and a presentation of the results obtained in this work, as well as a set of concluding remarks.

II. PHYSICAL MODEL

The context of this work is the study of jets in a steady-state regime. The steady-state jet model is an approximation in which it is assumed that all lines of the fluid (and thus the segments into which they are divided) share the same certain properties of light emission and velocity. As mentioned above, this study is centred in two basic models of the jet's shape, studied through their apparent luminosities.

The first approach is a simple cone-like model that represents the shape of a simple jet without an obstacle (see Figure 1a). The second model presents a conical jet model in contact with an obstacle. When the jet reaches the obstacle, the fluid is deflected and thus changes its geometry. This change is here modelled as a paraboloid figure (see Figure 1b). These models attempt to represent two different emitting flows, thus providing data to contrast the simple jet and the jet with the obstacle.

As mentioned before, these relativistic jets are studied as fluids. Therefore, they are divided into lines of emission, each one divided into segments that contribute to the total apparent luminosity observed at a certain angle.

The observed luminosity for zero redshift objects is

$$L_{app} = 4\pi d_L^2 F_{obs} \tag{1}$$

where d_L is the luminosity distance to the object and F_{obs} is the observed flux,

$$F_{obs} = \int I d\Omega \tag{2}$$

* Electronic address: victor.lopez.alv@gmail.com

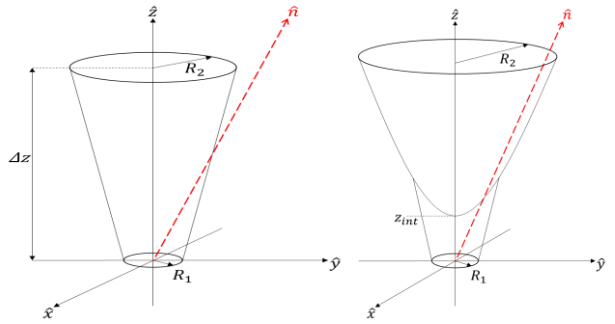

FIGS. 1a (left), 1b (right): representation of the models employed in this work. 1a corresponds to the simple cone-like jet model, 1b to the paraboloid jet.

Now, one can derive

$$I = \int j ds \tag{3}$$

where j is the volume emissivity in the direction of the observer ds is the distance measured along the ray within the source. $d\Omega = dA/d_L^2$, where A is defined as an element of area in the pattern frame that for a steady-state jet has zero velocity. Defining $dV = dA \cdot ds$, it is therefore obtained that

$$F_{obs} = \frac{1}{d_L^2} \int j dV \tag{4}$$

Using the Lorentz transformation formulae $j = D^3 j'$ and $V = V'/\gamma_i$, it is obtained that

$$L_{app} = 4\pi \frac{D^3}{\gamma_i} \int j' dV' \tag{5}$$

where D is the already mentioned Doppler factor,

$$D = [\gamma_i (1 - \beta \cos(\theta_{l.o.s.}))]^{-1} \tag{6}$$

Given our previous assumption that the emission of radiation is isotropic, it can be derived from (5) that $4\pi \int j' dV'$ is equal to the total emitted luminosity L', thus

$$L_{app} = \frac{D^3}{\gamma_i} L' \tag{7}$$

This will be the observed apparent luminosity of one segment, so to compute the total apparent luminosity of the full jet, every segment of every emission line has to be accounted for. All the previous equations and mathematical developments have been extracted from reference [6].

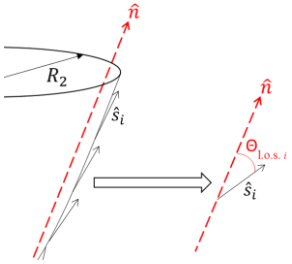

FIG. 2: Representation of the angle between the observer's orientation, defined by $\hat{n}$ and the direction of motion vector, $\hat{s}_i$. The angle formed by these vectors will be the angle defined $\theta_{l.o.s.}$.

As it is shown in Figure 2, every segment has a unique direction of motion, so will be at a different angle with the observer's line of sight – that is, a different $\cos(\theta_{l.o.s.})$. Thus, the Doppler factor of each segment will depend on its orientation.

The total amount of apparent luminosity, L_{app}, will be computed as follows

$$L_{app} = \sum_i \frac{D_i^3}{\gamma} L' \tag{8}$$

The calculations used in this work split the model in the same arbitrary number N of segments, where $N = m \cdot k$ (m being the number of radial divisions and k the number of circular fractions). The number of segments can be modified, for larger values of N more precise calculations will be obtained, but at the cost of higher computation time. The apparent luminosity of the emission line is then divided by the number of segments that form the line so that each segment has the same amount of emitted luminosity (as mentioned before, the assumption that each jet segment radiates isotropically in the flow frame).

The code behind the calculations first divides the structure of the jet in sections, and then computes each segment's position $\hat{s}_i = \frac{(r_i, \varphi_i, z_i)}{|\vec{s_i}|}$ changing from cylindrical coordinates to the cartesian axis coordinates using the following transformations:

$$\begin{aligned} x &= r\cos(\varphi) \\ y &= r\sin(\varphi) \\ z &= z \end{aligned} \tag{9}$$

In the conical jet model, this is a simple calculation, all that is needed is the final and initial coordinates of each line of emission to get the direction vector. Nevertheless, for the paraboloid model a more careful approach to the calculations is required.

The direction of motion vector will be computed by first finding the slope of the curve at the point location of the segment in question. Then taking into account the segment's coordinates in the cartesian frame, a second virtual point is added one unit beyond the straight line defined by its slope. Afterwards, both the virtual and point location vectors are subtracted, thus obtaining a new vector – *i.e.* the position vector. This position vector is then divided by its modulus to obtain a unitary vector.

This process is iterated throughout the whole line of emission, finding the total L_{app} of each line, and then iterated again to include all the emission lines to account for the total apparent luminosity of the jet, L_{app}.

After finding L_{app}, the set of calculations described above is conducted again for a different value of $\hat{n}$, the vector that defines the line of sight's angle with the z axis (the red line in Figure 2). The vector $\hat{n}$ expressed in spherical coordinates is:

$$\hat{n} = [\sin(\theta_{obs})\cos(\varphi), \sin(\theta_{obs})\sin(\varphi), \cos(\theta_{obs})] \tag{10}$$

To simplify the calculations, the azimuthal angle $\varphi = 0$, for it is an arbitrary angle and we can rotate the axis in order to make the polar angle move along the $y - z$ plane in cartesian coordinates.

All the calculations described above were for a given direction $\hat{n}$ of the observer's line of sight. To study the jet, this line of sight has to be computed for all its values to create a comprehensive display of the data obtained for every value of the $\cos(\theta_{los})$. Thus, $\hat{n}$ must be iterated N times for all the values of the polar angle $\theta_{obs} \epsilon \{0, \pi\}$.

Both models have similar parameters, but with evident differences in shape. The parameters used in the calculations are contained in the following tables:

R_1, radius of the lower base (pc)	0.01
R_2, radius of the upper base (pc)	1
Δz, height of the jet (pc)	10
L', emitted luminosity per segment (erg/s)	1

TABLE I: Parameters employed in the conical jet model calculations.

For the paraboloid jet model, new parameters will have to be defined:

R_1, radius of the lower base (pc)	0.01
Equation of the paraboloid z(r) (pc)	$z(r) = A \cdot r + z_0$
R_2, radius of the upper base (pc)	$R_2 = (\Delta z - z_0)/A$
Δz, height of the jet (pc)	10
L', emitted luminosity per segment (erg/s)	1

TABLE II: Parameters employed in the paraboloid jet model calculations.

In the equation of the paraboloid, A measures the curvature. The values for the curve will be $A = 4, 6$ and 8.

Besides these geometrical parameters, another parameter has to be taken into account: the velocity of the jet.

This velocity will be derived from γ, the Lorentz factor

$$\gamma = \frac{1}{\sqrt{1-\beta^2}} \qquad (11)$$

where $\beta = v/c$, and c is the speed of light in a vacuum.

Both the simple conical jet model and the paraboloid jet model have been studied for three values of the Lorentz factor: $\gamma = 1.1$, 3 and 10. The Lorentz factor is a dimensionless term that measures the relativistic nature of the system studied.

Typically, jets have apparent luminosities of $\sim 10^{40-47}$ erg/s, such as quasar 3C 273, with a measured $L_{app} \approx 4 \cdot 10^{47}$ erg/s [7]. In this work, the obtained results derive from representative parameters that aim not to provide an exact value of the apparent luminosity, but an evolution and study of the changes induced by the Doppler boosting effect in such apparent luminosity. The following results will present the change in the apparent luminosity of each model depending on its velocity and shapes.

III. RESULTS

As it has been previously discussed, the aim of this work is to provide a study on how the apparent luminosity of jets is affected by the Doppler boosting effect. The results here presented are the outcome of the calculations detailed in the previous section for different shapes and values of the Lorentz factor. The figures will be presented with the y-axis in a logarithmic scale, as the results differ in several orders of magnitude.

Figure 3 shows the jet in a mildly relativistic regime. In this case, the Lorentz factor corresponds to a velocity of

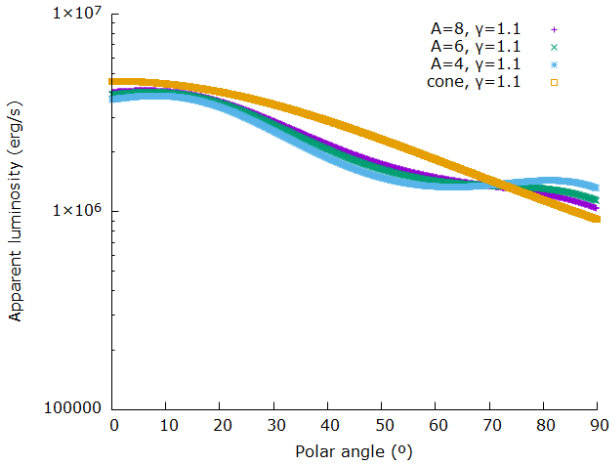

FIG. 3: Apparent luminosity in a logarithmic scale versus the polar angle of the observer. Comparison of the jet models with different values for A (the curve of the paraboloid model) for $\gamma = 1.1$.

$v \approx 0.42c$. It shows clearly how similar the observed apparent luminosity of the jet is for these two models in terms of magnitude, but it is interesting to observe how it varies with the angle. The curve for the paraboloid model is steeper due to its sudden change in the geometry, but in this case the slope of the paraboloid is not significant in terms of magnitude.

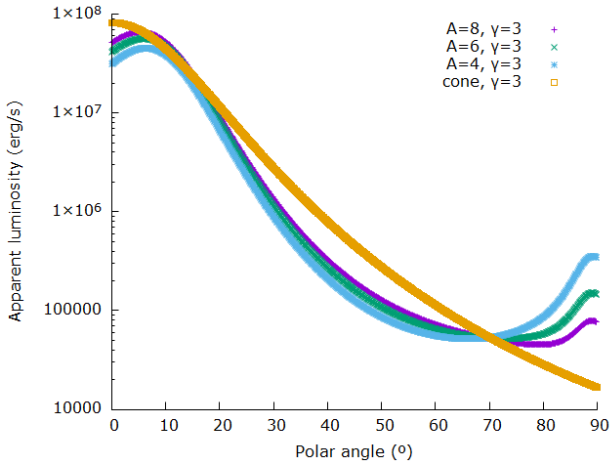

FIG. 4: Apparent luminosity in a logarithmic scale versus the polar angle of the observer. Comparison of the two jet models with different values of A (the curve of the paraboloid model) for $\gamma = 3$.

Figure 4 shows the jet for a Lorentz factor of $\gamma = 3$, so the fluid velocity is very relativistic: $v \approx 0.94c$. In this case, the results of the calculations show how the shape of the model becomes very relevant.

When the line of sight is directly upon the $\hat{z}$ axis (for polar angles between $\theta_{obs} = 0º$ and $\theta_{obs} \approx 0.5º$) the cone model emission is relatively constant, showing consistent values of the emitted radiation. Nonetheless, as soon as the observer's line of sight begins to move away from the

symmetry axis the apparent luminosity decreases several orders of magnitude.

In the case of the second model, however, the curvature of the paraboloid behaviour affects significantly the change of the apparent luminosity. For all three values of A, a peak is observed when the line of sight is in the same direction as the emission lines. Yet as soon as the polar angle changes, the apparent luminosity descends much faster than the parallel case of the cone model. This is due to the geometry of the jet. The surface of the paraboloid quickly changes its curvature, so there are fewer segments pointing in the same direction at any given section of this region. This causes the apparent luminosity to descend.

Moreover, there is a third significant region. It can be observed how when the line of sight reaches angles $\theta_{obs} > 80º$ the apparent luminosity rises in magnitude. This is due to the fact that when the jet reaches the obstacle, at the base of the paraboloid, the emission lines get deflected and thus light is radiated perpendicularly to the symmetry axis.

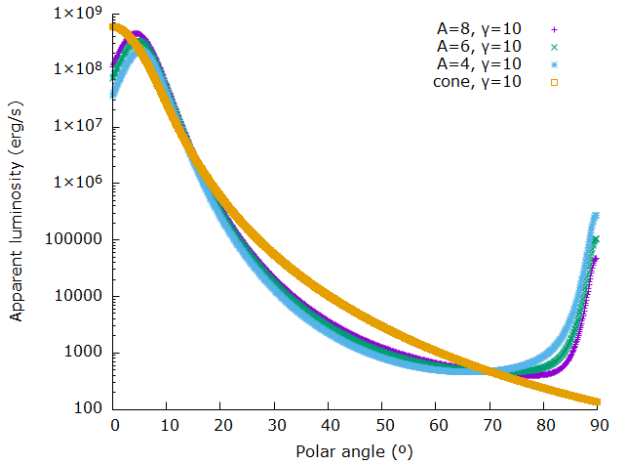

FIG. 5: Apparent luminosity in a logarithmic scale versus the polar angle of the observer. Comparison of the two jet models with different values of A (the curve of the paraboloid model) for $\gamma = 10$.

Figure 5 corresponds to a full relativistic regime. The Lorentz factor employed in this case is 10, so the velocity of the jet is $v \approx 0.995c$. The shape of the curves is significantly similar to the ones presented in Figure 4, but in this regime the different regions of emission are much more sharpen.

The Doppler boosting effect causes the regions of emission to radiate in a denser manner, and this is clearly seen in the third region of emission (for $\theta_{obs} > 80º$), where the apparent luminosity perceived by an external observer increases about $\sim 10^3$ erg/s compared to the central region.

In what follows, a comparison between the models is presented to explore the differences between steeper and smoother curvatures of the paraboloid. Figure 6 and Figure 7 attempt to show how the deviation from the cone model, the standard shape of a jet without an obstacle, is affected by a change in the geometry of the jet due to the deflection of the emission lines.

Figure 6 shows the results obtained for the paraboloid model. It is to be noticed how the two models have similar behaviours for the three Lorentz factor values $\gamma = 1.1$, $\gamma = 3$ and $\gamma = 10$. This resemblance in the magnitude of the emitted radiation makes the two models indistinguishable from one another until the third region of emission (for $\theta_{obs} > 80º$), where one can appreciate how the difference in apparent luminosity is significant for $\gamma = 3$ and $\gamma = 10$.

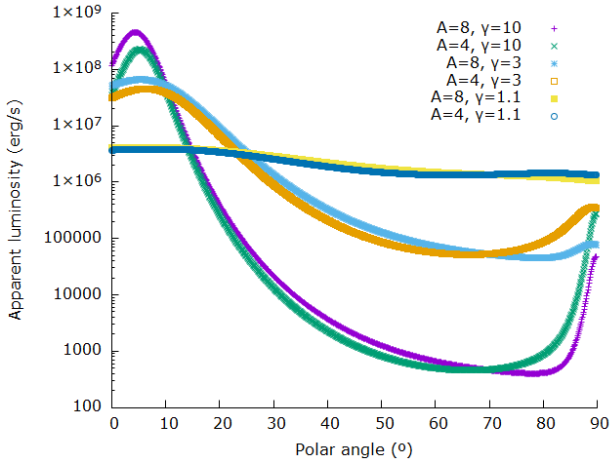

FIG. 6: Apparent luminosity in a logarithmic scale versus the polar angle of the observer. Comparison of two values of A, namely $A = 4$ and $A = 8$, for the different Lorentz factors used in this work.

As mentioned in section II, the paraboloid determined by the parameter $A = 8$ has the same upper base radius as the cone model ($R_2 = 1$ pc), and thus, this paraboloid is the most similar to the cone model for the jet. In Figure 7, both have been portrayed for the three Lorentz Factor values.

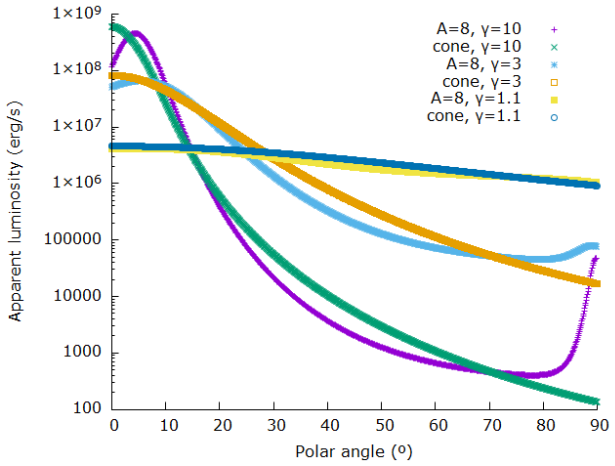

FIG. 7: Apparent luminosity in a logarithmic scale versus the polar angle of the observer. Comparison between the cone model and the paraboloid model for $A = 8$.

Several observations can be derived from Figure 7. First of all, it shows how similar the results are when the fluid velocity is mildly relativistic (for $\gamma = 1.1$). In this case, the Doppler factor is not significant enough to clearly allow an external observer (for any line of sight orientation) to determine if the jet has an obstacle in its path merely by measuring the jet's apparent luminosity. When the velocity of the jet increases and it becomes clearly relativistic (for $\gamma = 3$), a difference in magnitude will be observed if the orientation of the line of sight is in the third region of emission.

The difference between the cone model and the paraboloid model is relevant when the jet is in a highly

relativistic state (for $\gamma = 10$). As has been seen in the previous discussions of the results, there are two specially interesting regions of emission, the first one, close to the symmetry axis, and the third one, in the near-perpendicular polar angle.

When the symmetry axis is in line with the observer's angle, there is a clear difference in the behaviour of the apparent luminosity. In the case of the conical jet, as soon as the line of sight surpasses the lines of emission's direction of motion there is a decrease in the apparent luminosity. Whereas on the paraboloid model, the apparent luminosity of the jet model decreases a few degrees after the line of sight overcomes the curvature of the jet.

When in the third region of emission, the two models for the jet present another relevant difference as well. Namely, the three orders of magnitude that separate the apparent luminosity of the paraboloid jet model ($\sim 6 \cdot 10^5$ erg/s) from the conic jet model (~ 180 erg/s). This is, again, due to the Doppler boosting effect. The results obtained in this work lead to some observational conclusions being drawn.

IV. CONCLUSIONS

- First and foremost, a comparison between the models employed in this study has to be made. The cone model behaves fully as expected, presenting a consistent decrease in apparent luminosity when displacing the line of sight over the polar angle. For fully relativistic jets (as the one presented for $\gamma = 10$), the Doppler boosting effect will cause a steep decrease in apparent luminosity when moving out of the symmetry axis. Compared to the paraboloid model of the jet, it has to be stated that the difference is not very relevant for observers in line with the axis. This is due to the fact that the lines of emission are the same -*i.e.* the jet emits the same amount of radiation in both the paraboloid model and the cone model. The shape of the paraboloid can become relevant if the curvature is very smooth, for it will displace the peak of luminosity to larger angles, but it will also decrease its intensity, as seen in Figure 4 for $A = 4$.
- Under the assumptions made in this study, it is noticeable how big in terms of magnitude the difference of the radiated apparent luminosity is for different values of the Lorentz factor. As has been previously stated in the discussion of the results, this is due to the Doppler boosting effect, which reconducts the isotropically emitted radiation of the lines of emission into their direction of motion when the fluid is highly relativistic.
- It is also relevant to stress out that the jet loses luminosity when the line of sight angle moves away from the symmetry axis. This strongly suggests that it is difficult to observe relativistic jets from large distances when the observer is not in line with the jet's symmetry axis.
- There is another increase in apparent luminosity at the base of the jet in the second model, the paraboloid jet deviated due to an obstacle, observed when the polar angle is over $\theta_{obs} > 80º$). This is produced by the geometry of the system, which combined with the Doppler boosting effect, creates a second but less bright peak of luminosity. However, this is not strong enough to be observed at large distances, so only close observers will notice a paraboloid relativistic jet if placed at near perpendicular angles with its symmetry axis. This means that relativistic jets will be very difficult to observe outside the local universe if not directly aligned with the symmetry axis.

Acknowledgments

I would like to thank my advisor, Valentí Bosch-Ramón. This has not been the easiest semester, and his task-oriented behaviour has helped me get here. Amongst all the friends and family that are there for me every day (and those that without being here, are), I would like to thank especially my esteemed friend Raul Santiago Piera for his very much appreciated advise and encouragement. Thank you all.

[1] G. E. Romero, M. Boettcher, S. Markoff and F. Tavecchio, "Relativistic Jets in Active Galactic Nuclei," 2016.

[2] G. R. Blumenthal and R. J. Gould, «Bremsstrahlung, Synchrotron Radiation and Compton Scattering of High-Energy Electrons Travessing Dilute Gasses,» *Reviews of Modern Physics*, vol. 42, nº 2, pp. 237-244, 1970.

[3] V. Bosch-Ramon, «Non-thermal emission from standing relativistic shocks: an application to red giant winds interacting with AGN jets.,» *Astronomy & Astrophysics*, p. 1, 2015.

[4] M. Georganopoulos and J. G. Kirk, «The Beaming Pattern And Spectrum Of Radiation From Inverse Compton Scattering In Blazars,» *The Astrophysical Journal*, p. 1, 2001.

[5] M. H. Johnson and E. Teller, «Intensity Changes in the Doppler effect,» *Proceedings of the National Academy of Sciences of the United States of America (PNAS)*, 1981.

[6] M. Sikora, G. Madejski, R. Moderski and J. Poutanen, «Learning about Active Galactic Nucleus Jets From Spectral Properties of Blazars,» *The Astrophysical Journal*, nº 484, pp. 115-117, 1997.

[7] J. Kataoka, C. Tanihata, N. Kawai, F. Takahara, T. Takahashi, P. G. Edwards and F. Makino, «RXTE observations of 3C 273 between 1996 and 2000: variability time-scale and jet power,» *Monthly Notices of the Royal Astronomical Society*, vol. 336, nº 3, pp. 932-944, November 2002.